

Adsorption of fluid vesicles

A. Baumgärtner

Forum Modellierung, Forschungszentrum, 52425 Jülich, Germany

Somendra M. Bhattacharjee

Institute of Physics, Bhubaneswar 751 005, India

(Received 13 March 1997; accepted 29 May 1997)

The adhesion of fluid vesicles to a planar surface has been studied using Monte Carlo methods and scaling arguments for the random surface model. Deflated as well as inflated vesicles have been considered. Inflated vesicles, with internal pressure $p > 0$, exhibit with increasing adhesion strength a discontinuous conformational transition from unbound sphere-like conformations to strongly adsorbed two dimensional branched conformations. Deflated vesicles with $p = 0$ exhibit a continuous transition from three dimensional to two dimensional branched conformations where the type of transition is different from adsorption transition of branched polymers. The transition temperatures scale according to $\varepsilon_c/kT \sim p\sqrt{N}$, where N is the surface area of the vesicle. © 1997 American Institute of Physics. [S0021-9606(97)50533-2]

I. INTRODUCTION

The mechanisms and consequences of the adhesion of cells or vesicles to a substrate is of importance for our understanding of cell aggregation, proliferation and locomotion.¹ One of the basic differences between the adhesion of cells and vesicles is their adhesion mechanism, which is in the case of cells dominated by receptor-ligand interactions, whereas for vesicles classical forces as van der Waals and Coulomb are important. Although there are many additional differences between cells and vesicles, e.g. concerned with their internal structure, it is conceivable that they have some common features with regard to their conformational changes during adhesion processes. Therefore it is of interest to investigate certain models sharing some properties of cells and vesicles. The adhesion of such a model, which we call henceforth a vesicle, is the subject of the present paper.

The membranes of vesicles are approximately incompressible. Therefore they essentially do not change their area. Their shapes and related fluctuations are controlled by bending rigidity of the membrane²⁻⁴ and much less by their surface tension. Most of theoretical and experimental works on membrane adhesion have therefore been restricted to large bending rigidities, where thermal fluctuations are of only minor importance.⁵⁻⁷ Little is known about the behavior of adherent vesicles at low bending rigidity where the persistence length ξ_p is much smaller than the radius of the vesicle R , $\xi_p \ll R$. The persistence length⁸ is approximately $\xi_p = a_0 \exp[(4\pi/3)\kappa/kT]$, where a_0 is a microscopic length of the order of the monomer size and κ is the bending rigidity.

Besides the bending rigidity, the osmotic pressure difference $\Delta p \equiv p_{\text{in}} - p_{\text{out}}$ is another parameter which determines the shape of a vesicle. In particular, the combined effects of pressure and adhesion on the shapes of vesicles is of interest and will be the focus of the present work.

II. MODEL AND SIMULATION TECHNIQUES

As a model vesicle we used a fluid triangulated surface of spherical topology introduced recently,⁹ which has been investigated for the cases of internal pressure and bending rigidity.¹⁰ The present model surface is supposed to represent the bilayer membrane of real vesicles, however, restricted to the aspects of flexibility and tension. Effects related to the finite thickness of the membrane is here ignored, since actually the width of a membrane, about 4 nm, is very small compared to the radius of a vesicle which typically varies between 0.1 and 10 μm . Since we are primarily interested in the overall conformation of vesicles, our model surface can be considered as a simple first approximation to a flexible bilayer membrane.

A flexible triangular network is used as the simplest approximation of a flexible surface in three dimensional space. Each grid point on the mesh is connected by bonds with its neighboring points. The length of each bond is restricted to a certain range by a square-well potential, and the self-avoidance of the surface is implemented by introducing a hard sphere on each grid point. The diameter of the hard sphere, $\sigma = 1.0a$, is chosen such that the ratio of the diameter and the maximum bond length, $\ell_{\text{max}} = a\sqrt{2}$, disallows the self-penetration of the membrane. The microscopic length a , which defines the relation between our model membrane and the dimensions of a real membrane, will not be specified here, although general considerations would suggest that this length is in the order of the persistence length $a \approx \xi_p$, about 100 nm. Any attempt to displace a grid point is rejected if this causes overlaps of hard spheres, thus the surface is self-avoiding. The successive steps during the Monte Carlo procedure follows the usual Metropolis scheme. Select a grid point randomly or sequentially, displace it to a nearby location which is chosen at random. Then calculate the corresponding change in total energy δE (as defined below). The new location of the grid point is accepted if $\exp(-\delta E/kT) > \eta$, where $0 < \eta < 1$ is a random number, otherwise the old configuration is counted as the new one. Each

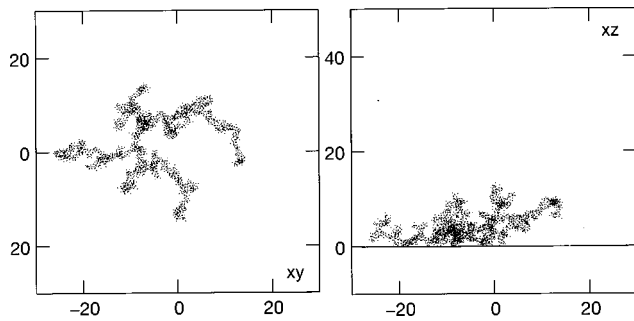


FIG. 1. Top view and side view snapshot of a deflated ($p=0$) vesicle at $\varepsilon/kT=1.0$ for $N=812$.

Monte Carlo step consists of N such attempts, where N is the total number of the grid points of the network.

The Monte Carlo steps described above are sufficient to simulate polymerized membranes and vesicles where the constituents of the surface are permanently connected to their neighbors. However, most membranes in biological system are fluid where the lipid molecules diffuse laterally in the plane of the membrane thereby continually changing their local environment. In order to account for this character of a membrane without going into the detailed realization of surface diffusion mechanism on the molecular level, one must adopt a much simpler and more abstract model suitable for numerical simulation. Combining the model of a flexible network with some kind of fluidity means, one has to relax the restriction on fixed connectivity, thus allow the grid points to exchange their neighbors, and at the same time, preserve the topology and the integrity of the structure. In a triangular mesh, this can be accomplished by the following mechanism (“dynamic triangulation”).^{9,11}

Select a pair of grid points randomly or sequentially such that they are the respective vertices of two triangles which share the same edge, then perform a bond-exchange step if the following conditions are satisfied: 1) these two points are not directly connected yet; 2) the numbers of direct-connected neighbors of the two vertices of the common edge are both greater than the minimum allowed number (say, 3); 4) The distance between these two points are within the interval of the acceptable bond length $\ell_{\max} = \sqrt{2}$. If all these conditions are satisfied, the new bond between these two points is created and the bond of the common edge of the two triangles is removed. In this bond-exchange procedure, the total numbers of bonds and triangles are preserved, so is the two dimensional topology of the membrane which is the essential of the structure. The advantage of this simple procedure is its locality, only the local connections are rearranged and the cumulative effects of the bond-exchange and grid point displacement allow the grid points to have more freedom to move in space, not just a restricted diffusion in 3-D as in the case of fixed-connected mesh but also in the 2-D surface itself. In fact, within certain number of steps, each grid point would have the opportunity of being connected with any other point and this resembles the fluidity of the system. It should be noted that during the process of dynamic triangulation the volume of the vesicle is

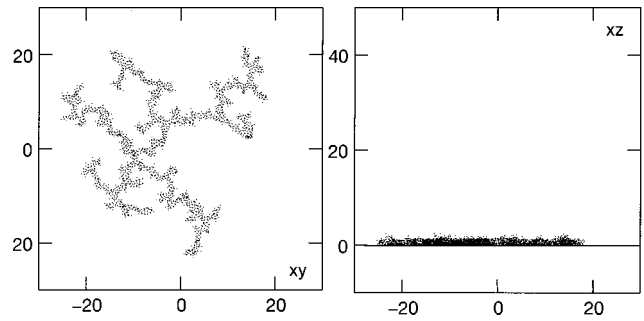


FIG. 2. Top view and side view snapshot of a deflated ($p=0$) vesicle at $\varepsilon/kT=4.0$ for $N=812$.

changed, and hence at each triangulation step the Metropolis criterion has to be applied in order to accept or reject the new volume according to $\exp(-p\delta V/kT) > \eta$ or $< \eta$, respectively, where $p \equiv \Delta p a^3/kT$ and δV is the change of the volume.

The adhesion between the surface of the vesicle and the flat substrate is represented by a short range attractive potential of square-well type

$$V(z) = -\varepsilon/(1+z)^2, \quad \text{for } 0 < z < w, \quad (1)$$

where $V(z) = \infty$ for $z < 0$ and $V(z) = 0$ for $z > w$. The parameter w is a cut-off, which has been introduced in order to model a contact potential in the present continuum model. Obviously, for large w , say in the order of the size of the vesicle, the inner surface of the vesicle would be attracted also, which is not of interest. Therefore we have limited the range of the potential to $z \leq w = 0.57$, where the upper limit is the closest distance two fluid surfaces of the present type can approach each other without violating the excluded volume conditions.

Since for finite sizes N of the vesicles and due to the finite range of the attractive potential the probability of the vesicle to escape from the attractive range at any temperature is nonzero, we have restricted the motion of the vesicle to the extent that at least one monomer of its surface must be found at coordinate $z < w$.

In determining the averages we have used 10^6 Monte Carlo steps.

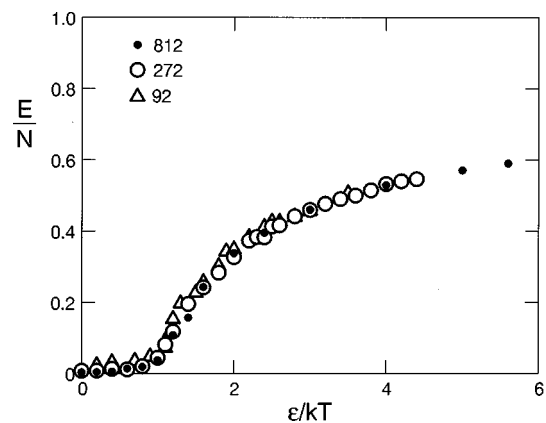


FIG. 3. Adhesion energy E/N versus adsorption strength ε/kT at zero pressure for vesicles sizes $N=92, 272, 812$.

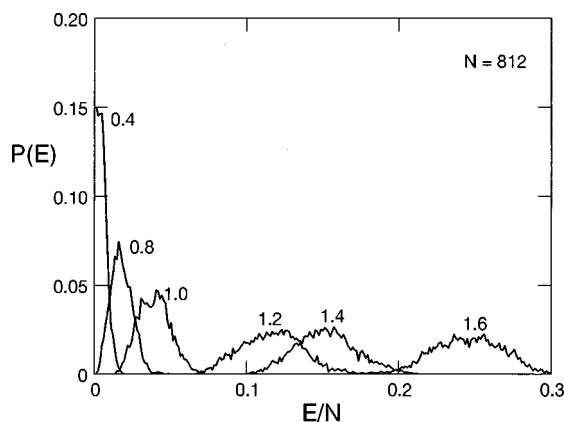


FIG. 4. Probability distribution of energy $P(E)$ for various values of ϵ/kT at zero pressure for vesicles of size $N=812$.

III. RESULTS AND DISCUSSIONS

A. Deflated vesicles

In the following subsection we report on our results on the adsorption of “deflated” ($p=0$) vesicles. Since it is known that deflated vesicles exhibit conformations of branched structures,^{10,12} where the mean square radius of gyration and the volume are proportional to the surface area, $R^2 \sim V \sim N$, one might expect a situation comparable to the case of the adsorption of branched polymers to impenetrable surfaces.¹³ However, since branched vesicles differ from branched polymers with respect to the conservation of their topology, i.e., branched vesicles can be considered as the annealed analogon of branched polymers with quenched topologies, it is conceivable that some statistical quantities such as crossover exponents¹³ are different in the two models.

Typical snapshots of deflated vesicles are depicted in Figs. 1 and 2, for weak and strong adsorption, respectively. They clearly demonstrate the transition from a weakly bound to a strongly bound state and between the three-dimensional and the two-dimensional branched structure of the vesicle. We have estimated the contact energy E , which is defined as the number of monomers of the vesicle found in the interval

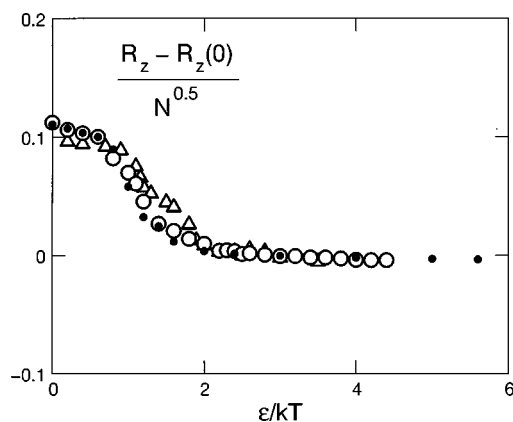


FIG. 6. Scaled vertical size R_z versus ϵ/kT at zero pressure for vesicles of various sizes.

$0 < z < w$. The contact energy per bead E/N as a function of the adsorption strength ϵ/kT is presented in Fig. 3. The transition point is located at $\epsilon_c/kT \approx 1$. Interestingly, finite size effects are very small although the surface area N changes by a factor of 9. This is in contrast to branched polymers¹³ where the critical adsorption temperature T_c depends significantly on the size according to $T_c(N) = T_c(\infty) - BN^{-0.7}$. Recently a first order transition has been proposed for the adsorption of branched model vesicles on lattices.¹⁴ Whether the present transition is also of first order has been examined by looking at the probability distribution of energy $P(E)$. In case of a discontinuous transition one would expect close to the transition point a bimodal distribution of the energy E . In Fig. 4 the distribution $P(E)$ is presented for various values of ϵ/kT . At least for $\epsilon/kT=1.0$ and 1.2 , there is no evidence of a bimodal shape and hence no discontinuity of the energy.

The continuity of the transition is further corroborated by the change of the conformation of the vesicles as a function of adhesion strength. The average vertical size R_z and the average parallel size R_{xy} are presented in Figs. 5–7. The data of the vertical size, as presented in Fig. 5, exhibit a continuous transition between a weakly adsorbed state at $\epsilon < \epsilon_c$ and a strongly adsorbed state at $\epsilon/kT > \epsilon_c/kT$ where R_z is independent of N . Below the transition point R_z is

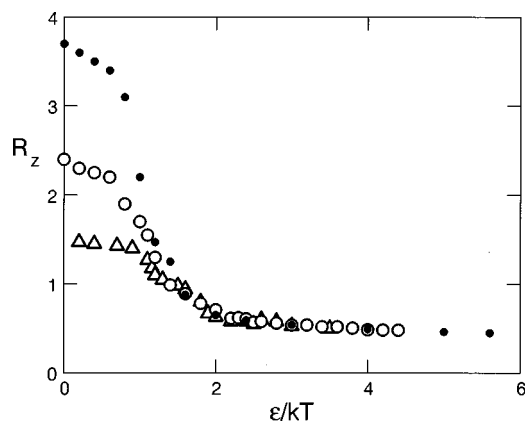


FIG. 5. Average vertical size R_z versus ϵ/kT at zero pressure for vesicles of various sizes.

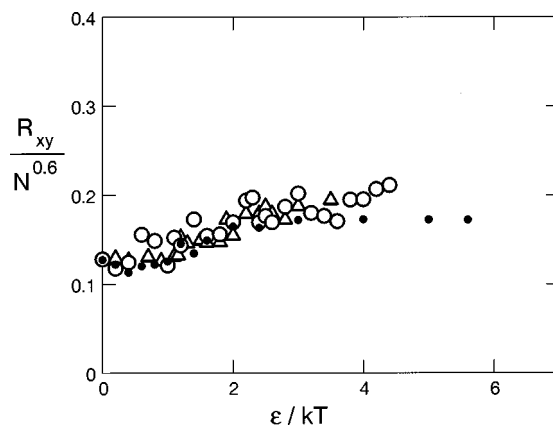


FIG. 7. Scaled parallel size R_{xy} versus ϵ/kT at zero pressure for vesicles of various sizes.

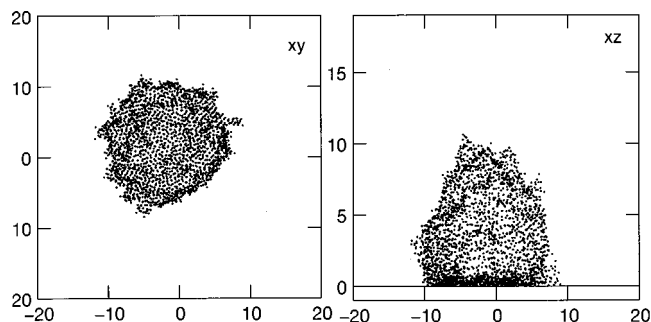


FIG. 8. Top view and side view snapshot of weakly adsorbed inflated vesicle at $p=0.26$, $\varepsilon/kT=2.9$ for $N=812$.

expected to scale according to $R_z \sim \sqrt{N}$ corresponding to a three dimensional branched vesicle. This is demonstrated in Fig. 6 for

$$R_z - R_z(0) = N^{0.5} f(kT/\varepsilon). \quad (2)$$

where we have assumed $f(x) \approx 0$ and $R_z(x) = 0.55$ for $x < 1$.

The average parallel size R_{xy} is presented in Fig. 7. The data indicate that the spreading of the vesicle on the surface is a continuous process where $R_{xy} = A(T)N^{0.6}$ and the prefactor $0.1 < A(T) < 0.2$ is a weak function of temperature. The exponent of 0.6 is, as expected, in agreement with the well known case of two dimensional branched polymers.¹⁵ However, our data are not sufficiently precise in order to observe the conformational transition in R_{xy} between two dimensional branched vesicles of $R_{xy} \sim N^{0.6}$ at $\varepsilon > \varepsilon_c$ and three dimensional branched vesicles $R_{xy} \sim N^{0.5}$ at $\varepsilon < \varepsilon_c$. It seems likely that much large vesicles would exhibit a more clear picture.

Previous studies on the adsorption of branched vesicles on lattices¹⁴ have reported on a second conformational transition with increasing adhesion strength from two dimensional branched conformations to disc-like conformations. In the latter case a vesicle is thought to be spread compactly on the plane, similar as for two dimensional self-avoiding ring polymers¹⁶ where $R_{xy} \sim N^{0.75}$. Although there is no evidence for such a transition in our present simulations we cannot exclude that for much larger vesicles this second type of branched-compact transition in two dimensions would take place.

B. Inflated vesicles

In the following subsection we report on our results on the adsorption of ‘‘inflated’’ ($p > 0$) vesicles. This situation is different from the previous one since at low adhesion strength the vesicles are inflated provided the pressure is larger than a threshold value¹⁰ in the order of $p^* \sim N^{-1/2}$. A snapshot of such a situation is depicted in Fig. 8. With increasing ε/kT the vesicle becomes more flat until it spreads out on the surface undergoing a transition to a two-dimensional branched structure as depicted in Fig. 9. This spreading transition is discontinuous and exhibits a considerable hysteresis of the energy as a function of ε/kT . Similar

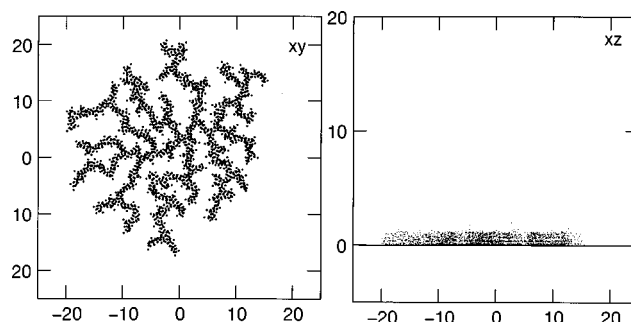


FIG. 9. Top view and side view snapshot of a strongly adsorbed inflated vesicle at $p=0.26$, $\varepsilon/kT=9.0$ for $N=812$.

behavior is also observed for R_z and R_{xy} . In Fig. 10 the hysteresis of the adhesion energy is presented. The width of the hysteresis loop depends as usual on the successive cooling and heating rate. Since we could not totally suppress the hysteresis effect by performing very long simulation runs, we have located the expected transition point for infinitely slow cooling and heating rate symmetrically between the two transition points according to successive cooling and heating series as depicted in Fig. 10. According to this procedure we have estimated the critical adhesion strength ε_c/kT as a function of the scaled pressure $p\sqrt{N}$ which is shown in Fig. 11. At $p\sqrt{N} \gg 1$ the transition line is linear,

$$\varepsilon_c/kT \approx \frac{1}{3} p\sqrt{N}, \quad (3)$$

whereas for $p\sqrt{N} \rightarrow 0$ a crossover to the special transition at $p=0$, as discussed in the previous section, is expected.

The average perpendicular sizes R_z of the vesicles as a function of adhesion strength and pressure is shown in Fig. 12. Since the critical adhesion strength scales according to $\varepsilon/kT \sim p\sqrt{N}$, the appropriate scaling variable is $\varepsilon/p\sqrt{N}$. Below ε_c/kT the vesicle is inflated and hence the perpendicular size scales with the surface area similar as for a sphere, $R_z \sim \sqrt{N}$. Below the transition point the vesicles are flat. (It should be noted that the data of R_z above the transition point, as depicted at the right hand side of Fig. 12, have been reduced by a factor of 100 in order to fit to the scale of the

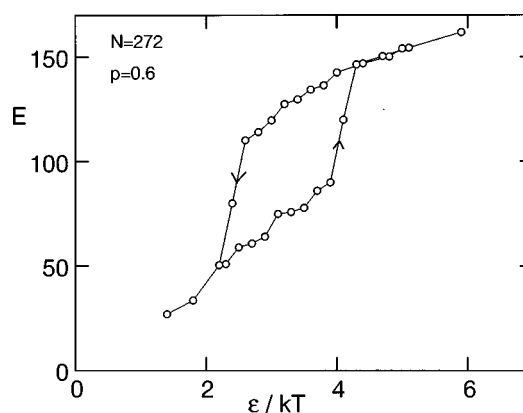


FIG. 10. Hysteresis of adhesion energy as a function of adhesion strength ε/kT .

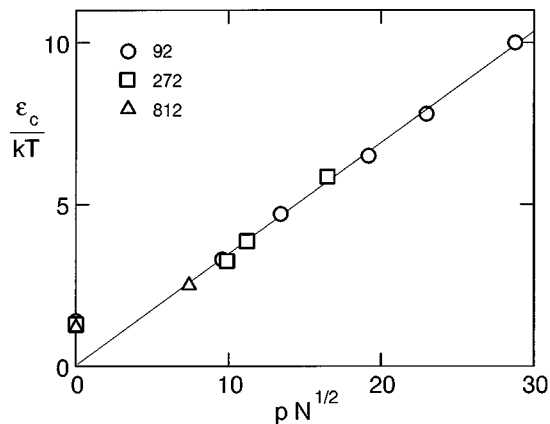


FIG. 11. Phase diagram of adhesive vesicles.

figure.) For $\varepsilon > \varepsilon_c$ the vesicles are two dimensional and have an average thickness in the range of $0.4 < R_z < 0.6$.

The effective scaling of the parallel component R_{xy} is presented in Fig. 13. At low adhesion strength (left part of the figure) the parallel component scales as expected for a spherical object proportional to the perpendicular component according to $R_{xy} \sim R_z \sim \sqrt{N}$. However, in order to obtain a satisfactory overlap of the data we have introduced a weak dependence on the pressure, approximately $R_{xy} \sim p^{0.14}$. This pressure dependence may be attributed to deviations from a spherical shape with increasing adhesion strength ε/kT . Above the adhesion threshold the vesicle is strongly adsorbed and flat. The two dimensional structures are comparable to those of branched polymers. Therefore the parallel component scales accordingly to $R_{xy} \sim N^{0.6}$. The exponent compares well with the estimate 0.61 for branched polymers.¹⁵

The effective scaling of the volume is presented in Fig. 14. The best collapse of the data are obtained for $V \sim N^{1.7} p^{0.4}$ below the adhesion threshold, and $V \sim N$ above. The latter result is as expected, since for the branched structures the volume must be proportional to the surface area.

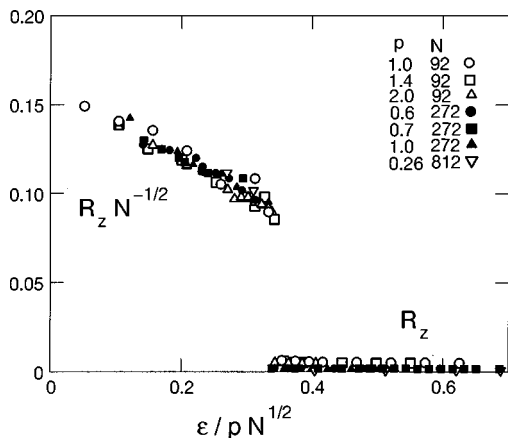


FIG. 12. Scaled vertical size R_z versus $\varepsilon/p\sqrt{N}$ below and above the critical adhesion strength ε_c for vesicles of various sizes. The data of R_z above the transition point (right hand side of the figure) have been reduced by a factor of 100 in order to fit to the scale of the figure.

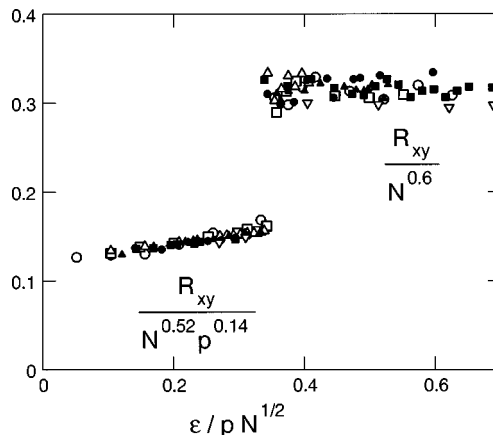


FIG. 13. Scaled parallel size R_{xy} versus $\varepsilon/p\sqrt{N}$ below and above the critical adhesion strength ε_c for vesicles of various sizes. The data of $R_{xy}/N^{0.6}$ as presented at the right hand side of the figure have been shifted by 0.15 upwards in order to separate from the data at the left hand side of the figure.

The result at $\varepsilon < \varepsilon_c$ is somewhat surprising, because the volumes of inflated vesicles increase faster than the expected behavior of spherical objects, $V \sim N^{1.5}$. However, this result is in reasonable agreement with previous simulations on inflated vesicles. For the present continuum model vesicle¹⁰ it has been found $V \sim N^{1.75} p^{0.5}$, whereas for a lattice model¹² it has been reported $V \sim N^{1.8} p^{0.6}$. The deviation from the expected ordinary spherical shape have been explained based on a generalized¹⁰ blob picture of de Gennes¹⁶⁻¹⁸ and similarly by a generalization of Pincus' result¹⁹ for stretched polymer chains.¹²

The effective scaling of the adhesive contact energy is presented in Fig. 15. Since the data scatter too much in the low adhesion regime we cannot exclude that in both regimes the leading powers in N and p are the same. However, according to the data we obtain a slight difference, $E/Np^{0.5} = g_E(x)$ at $\varepsilon < \varepsilon_c$, whereas $E/N^{1.15} p^{0.3} = f_E(x)$ at $\varepsilon > \varepsilon_c$, and different scaling functions $g_E(x)$ and $f_E(x)$ with $x = \varepsilon/p\sqrt{N}$.

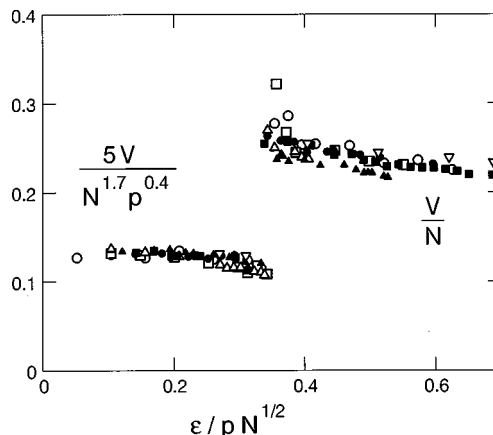


FIG. 14. Scaled volume V versus $\varepsilon/p\sqrt{N}$ below and above the critical adhesion strength ε_c for vesicles of various sizes.

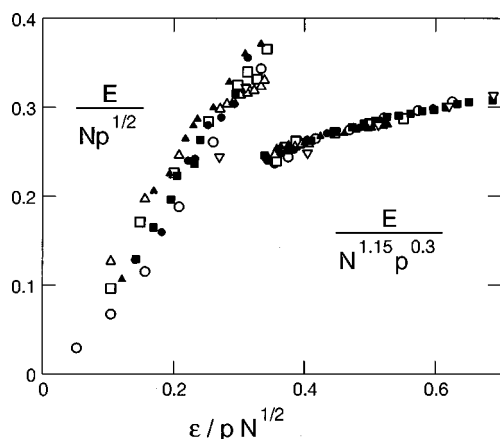


FIG. 15. Scaled energy E versus $\varepsilon/p\sqrt{N}$ below and above the critical adhesion strength ε_c for vesicles of various sizes.

IV. CONCLUSIONS

In summary, we have investigated the adhesion of fluid vesicles to a planar impenetrable surface using Monte Carlo methods. As a model vesicle we have studied the random surface model. In the case of deflated vesicles with internal pressure $p=0$ we have found a continuous transition between three dimensional and two dimensional branched conformations. The transition temperature is independent of the size of the vesicles, and hence different from the adsorption transition of branched polymers. In the case of inflated vesicles with internal pressure $p>0$ we have found a discontinuous transition between the high temperature state, where the vesicles exhibit a spherical inflated shape, and the low

temperature state, where the vesicle is strongly adsorbed exhibiting two dimensional branched conformations.

Disc-like two dimensional conformations, which have been reported recently for strongly adhesive vesicles on lattices,¹⁴ have not been detected for the present continuum model.

ACKNOWLEDGMENT

Financial support by the Indo-German project 1L3A2B is gratefully acknowledged.

- ¹G. I. Bell, M. Dembo, and P. Bongrand, *Biophys. J.* **45**, 1051 (1984).
- ²P. B. Canham, *J. Theor. Biol.* **26**, 61 (1970).
- ³W. Helfrich, *Z. Naturforsch.* **28c**, 693 (1973).
- ⁴E. A. Evans, *Biophys. J.* **14**, 923 (1974).
- ⁵E. Bouchaud and J. P. Bouchaud, *J. Phys. (Paris)* **50**, 829 (1989).
- ⁶U. Seifert and R. Lipowsky, *Phys. Rev. A* **42**, 4768 (1990).
- ⁷U. Seifert, *Phys. Rev. Lett.* **74**, 5060 (1995).
- ⁸L. Peliti and S. Leibler, *Phys. Rev. Lett.* **54**, 1690 (1985).
- ⁹A. Baumgärtner and J.-S. Ho, *Phys. Rev. A* **41**, 5747 (1990); J.-S. Ho and A. Baumgärtner, *Europhys. Lett.* **12**, 295 (1990).
- ¹⁰G. Gompper and D. Kroll, *Phys. Rev. A* **46**, 7466 (1992); *Phys. Rev. E* **51**, 514 (1995).
- ¹¹J.-S. Ho and A. Baumgärtner, *Mol. Simul.* **6**, 163 (1991).
- ¹²A. Baumgärtner, *Physica A* **190**, 63 (1992); *J. Chem. Phys.* **98**, 7496 (1993).
- ¹³L. Lam and K. Binder, *J. Phys. A* **21**, L405 (1988).
- ¹⁴E. Orlandini, A. L. Stella, M. C. Tesi, and F. Sullivan, *Phys. Rev. E* **48**, R4203 (1993).
- ¹⁵G. Parisi and N. Sourlas, *Phys. Rev. Lett.* **46**, 871 (1981).
- ¹⁶A. C. Maggs, S. Leibler, M. E. Fisher, and C. J. Camacho, *Phys. Rev. A* **42**, 691 (1990).
- ¹⁷P. G. de Gennes, *Scaling Concepts in Physics* (Cornell University Press, Ithaca, 1979).
- ¹⁸R. Lipowsky and A. Baumgärtner, *Phys. Rev. A* **40**, 2078 (1989).
- ¹⁹P. Pincus, *Macromolecules* **9**, 386 (1976).